POSITIVE TOPOLOGICAL ENTROPY OF CHUA'S CIRCUIT: A COMPUTER ASSISTED PROOF

ZBIGNIEW GALIAS*

*Department of Electrical Engineering, University of Mining and Metallurgy,
al. Mickiewicza 30, 30-059 Kraków, Poland*

In this paper we describe a technique for proving that a particular system is chaotic in the topological sense, i.e. that it has positive topological entropy. This technique combines existence results based on the fixed point index theory and computer-assisted computations, necessary to verify the assumptions of the existence theorem. First we present an existence theorem for periodic points of maps, which could be appropriately homotoped with the deformed horseshoe map. As an example we consider Chua's circuit. We prove the existence of infinitely many periodic points of Poincaré map associated with Chua's Circuit. We also show how to use this result to prove that the topological entropy of the Poincaré map and also of the continuous system is positive.

1. Introduction

Chaotic behavior is observed in laboratory experiments and simulations of many nonlinear systems. They are believed to be chaotic, but there is still a lack of rigorous mathematical proofs of existence of chaos in particular systems. In this paper we describe a general method for proving the existence of chaos in dynamical systems. This technique can be used to prove the existence of an infinite number of periodic orbits for a given system and also to show that its topological entropy is positive. For systems with these two properties there exist trajectories with very complicated behavior.

Recently Zgliczyński [1996] proved the existence of an infinite number of periodic orbits for maps which could be appropriately homotoped with the horseshoe map. Here we present a modification of this theorem for maps with a deformed horseshoe embedded. This approach is different from the approach via Shilnikov's theorem (compare [Chua

et al., 1986]), where one can prove the existence of a homoclinic orbit and a horseshoe embedded in its neighborhood. From that, one can conclude the existence of infinitely many periodic orbits, but only for some unknown parameter values within a certain range. There is however no general method to prove the existence of a horseshoe and an infinite number of periodic orbits for given values of parameters. Our method has the advantage that it allows to prove the existence of infinitely many periodic orbits and positivity of topological entropy for fixed values of parameters.

In Sec. 2 we introduce the notion of the fixed point index, horseshoe map and present main mathematical results. In Sec. 3 we describe an application of the theorems from Sec. 2 for Chua's circuit. We prove rigorously, using interval arithmetic, that a deformed horseshoe is embedded within the Poincaré map and that there exist infinitely many periodic orbits for Chua's circuit. In Sec. 4 we show

---

*E-mail: galias@zet.agh.edu.pl

how to prove that the topological entropy of the system is positive. In Sec. 5 we compare theoretical results obtained for Chua's circuit with simulation results. We find several other periodic orbits, showing that the behavior of Chua's circuit is even more complicated than the behavior of a deformed horseshoe map. In conclusions we discuss the limitations and possible generalizations of this technique.

2. Infinite Number of Periodic Orbits

The existence theorem is based on the results of Zgliczyński [1996]. The general method is to construct an appropriate homotopy connecting the considered map with the (deformed) horseshoe map. This allows one to prove the existence of at least as many periodic orbits as for the horseshoe map. Let us first describe the notion of the fixed point index and introduce the definition of the (deformed) horseshoe map.

2.1. *Fixed point index*

The fixed point index theory we use was developed by Dold [1980]. By $\mathbb{R}$ and $\mathbb{Z}$ we denote sets of real and integer numbers respectively. If U is a subset of $\mathbb{R}^n$ we use the notation ∂U, $\overline{U}$ and $\text{int} U$ for the boundary, closure and the interior of U respectively.

Let $\mathcal{G}$ denote the class of pairs (f, U) such that $f : V \mapsto \mathbb{R}^n$ is a continuous map, U is an open and bounded set such that $\overline{U} \subset V \subset \mathbb{R}^n$ and f has no fixed points on ∂U, i.e. $\text{Fix} f \cap \partial U = \emptyset$ where

$$\text{Fix} f \stackrel{\text{df}}{=} \{\mathbf{x} \in V : f(\mathbf{x}) = \mathbf{x}\}. \tag{1}$$

Usually the fixed point index is introduced using algebraic topology (compare [Dold, 1980; Granas, 1972]). We will give an axiomatic definition of the fixed point index.

Definition 1. The *fixed point index* is an integer valued function $I : \mathcal{G} \mapsto \mathbb{Z}$ satisfying the following axioms:

(1) if W is an open set such that $\text{Fix} f \cap U \subset W \subset U$, then $I(f, U) = I(f, W)$,
(2) if f is constant then $I(f, U) = 1$ if $f(U) \in U$ and $I(f, U) = 0$ if $f(U) \notin U$,
(3) if U is a union of a finite number of open sets U_i, $i = 1, \ldots, m$, such that $U_i \cap U_j \cap \text{Fix} f = \emptyset$ for $i \neq j$, then $I(f, U) = \sum_{i=1}^{m} I(f, U_i)$,

(4) if $f : V \mapsto \mathbb{R}^n$, $f' : V' \mapsto \mathbb{R}^m$ are continuous maps and (f, U), (f', U') belong to the class $\mathcal{G}$ (i.e. $\text{Fix} f \cap \partial U = \emptyset$, $\text{Fix} f' \cap \partial U' = \emptyset$), then $I(f \times f', U \times U') = I(f, U) I(f', U')$, where $f \times f' : V \times V' \mapsto \mathbb{R}^{n+m}$,
(5) if $F : V \times [0, 1] \mapsto \mathbb{R}^n$ is a homotopy,[1] $\overline{U} \subset V$ and $\text{Fix} F_t \cap \partial U = \emptyset$ for every $t \in [0, 1]$ then $I(F_0, U) = I(F_1, U)$.

For the proof of existence of function I satisfying the above axioms, see [Granas, 1972] or [Dold, 1980]. For a not necessarily open set N such that $\overline{N} \subset V \subset \mathbb{R}^n$ by index $I(f, N)$, we will denote the fixed point index of f with respect to the interior of N, i.e. $I(f, N) \stackrel{\text{df}}{=} I(f, \text{int} N)$.

Let us recall the property of the fixed point index, which states the existence of a fixed point, if the fixed point index is non-zero.

Remark 1. Let $f : V \mapsto \mathbb{R}^n$ be a continuous map, U — an open bounded set such that $\overline{U} \subset V \subset \mathbb{R}^n$. Let us assume that $\text{Fix} f \cap \partial U = \emptyset$. If $I(f, U) \neq 0$ then $\text{Fix} f \cap U \neq \emptyset$,

Proof. This is a simple conclusion from part 3 of Definition 1. ∎

The fixed point index for a linear map can be easily computed (compare [Dold, 1980]). Let $f : \mathbb{R}^n \mapsto \mathbb{R}^n$ be a linear map. The set $\text{Fix} f$ is compact if and only if $+1$ is not an eigenvalue of f. In such a case $\mathbf{0} \in \mathbb{R}^n$ is the only fixed point of f and the fixed point index of f with respect to an arbitrary neighborhood U of $\mathbf{0}$ is equal to

$$I(f, U) = (-1)^\eta, \tag{2}$$

where η is a number of real eigenvalues λ of f such that $\lambda > 1$.

2.2. *Horseshoe map*

Let $N_0 = [-1, 1] \times [-1, -0.5]$, $N_1 = [-1, 1] \times [0.5, 1]$. Let $P = [-1, 1] \times \mathbb{R}$ be the smallest vertical stripe containing N_0 and N_1. Let $M_- = [-1, 1] \times (-\infty, -1)$, $M_0 = [-1, 1] \times (-0.5, 0.5)$, $M_+ = [-1, 1] \times (1, \infty)$. M_-, M_0 and M_+ are subsets of

---

[1]If X, Y are topological spaces and $[0, 1]$ denotes the unit interval, then a continuous map $F : X \times [0, 1] \mapsto Y$ is called a *homotopy* (of X into Y). For every $t \in [0, 1]$ the map $F_t : X \mapsto Y$, $F_t(x) \stackrel{\text{df}}{=} F(x, t)$ is continuous.
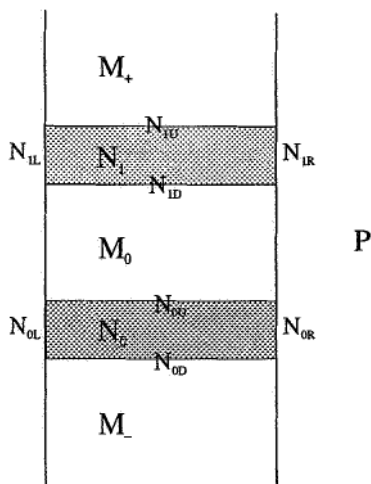
Fig. 1. Sets N_0, N_1, M_-, M_0 and M_+.

P lying below, between and above N_0, N_1. Let N_{0D}, N_{0U} be the lower and upper horizontal edges and N_{0L}, N_{0R} be the left and right vertical edges of N_0, and similarly N_{1D}, N_{1U}, N_{1L}, N_{1R} be the lower, upper, left and right edges of N_1 (i.e. $N_{0D} = [-1, 1] \times [-1, -1]$, $N_{0L} = [-1, -1] \times [-1, -0.5]$, etc). Sets defined above are shown in Fig. 1.

The horseshoe map (Smale's horseshoe) is a map linear on N_0 and N_1 defined by:

$$h_s(x, y) \stackrel{\mathrm{df}}{=} \begin{cases} \left(\frac{1}{4}x - \frac{1}{2}, \pm 5\left(y + \frac{3}{4} \right) \right) \\ \qquad \text{for } (x, y) \in N_0 \,, \\ \left(\frac{1}{4}x + \frac{1}{2}, \pm 5\left(y - \frac{3}{4} \right) \right) \\ \qquad \text{for } (x, y) \in N_1 \,. \end{cases} \quad (3)$$

Images of rectangles N_0 and N_1 under h are shown in Fig. 2(a). From the definition of h_s it is clear that images of horizontal edges of rectangles N_0 and N_1 lie above N_1 or below N_0. Signs of the coefficients determine positions of that images in the following way: If the coefficient in the first equation is $+5$, then $h_s(N_{0D}) \subset M_-$, $h_s(N_{0U}) \subset M_+$, if this coefficient is -5, then $h_s(N_{0D}) \subset M_+$, $h_s(N_{0U}) \subset M_-$. Similarly the sign in the second equation changes positions of sets $h_s(N_{1D})$ and $h_s(N_{1U})$ with respect to the sets N_0 and N_1.

Using the linearity of the horseshoe map it is possible to give the number of periodic points with a given period and to compute corresponding fixed point indices. Let us choose a natural number n, and a sequence $(a_0, \ldots, a_{n-1})$ with elements from the set $\{0, 1\}$. As the horseshoe is linear on N_0, N_1 and each of the images $h_s(N_0)$, $h_s(N_1)$ covers sets N_0, N_1 vertically, then it is clear that there exists a periodic point $\mathbf{x}$ of h_s with period n ($h_s^n(\mathbf{x}) = \mathbf{x}$) such that its trajectory follows sequence $(a_0, \ldots, a_{n-1})$ (i.e. $h_s^i(\mathbf{x}) \in N_{a_i}$ for $i = 0, 1, \ldots, n - 1$. The Jacobian of h_s^n at $\mathbf{x}$ is equal to

$$\mathbf{J} = \begin{pmatrix} 0.25^n & 0 \\ 0 & \pm 5^n \end{pmatrix}. \quad (4)$$

$+1$ is not an eigenvalue of $\mathbf{J}$. Hence there exists a neighborhood U of point $\mathbf{x}$, which does not contain ⁀er fixed points of h_s^n. From Eq. (2) the fixed ⁀t index of the pair (h^n, U) is non-zero. Because ⁀rent sequences $(a_0, \ldots, a_{n-1})$ lead to different fixed points of h_s^n and there are 2^n such sequences for given n, we conclude that there exist 2^n different fixed points of the map h_s^n.
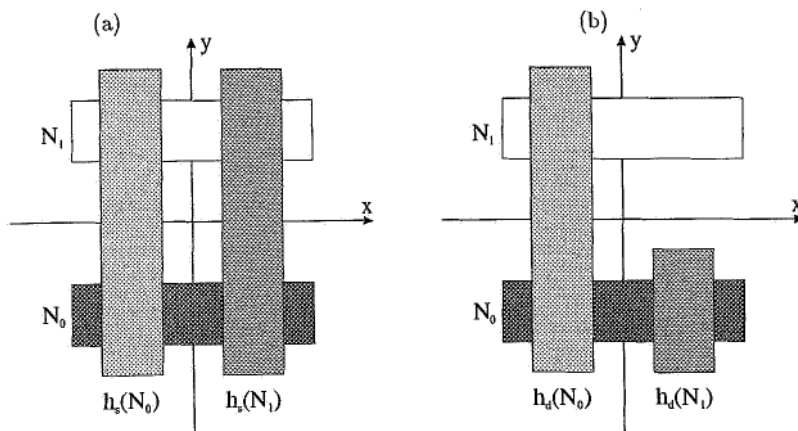

Fig. 2. Sets N_0, N_1 and their images under (a) horseshoe map, (b) deformed horseshoe map.

2.3. *Deformed horseshoe map*

The deformed horseshoe map h_d is a map linear on N_0 and N_1. For $(x, y) \in N_0$ the definition of h_d is the same as the definition of the original horseshoe map, but for $(x, y) \in N_1$ the stretching action is weaker:

$$
h_d(x, y) \stackrel{\text{df}}{=} \begin{cases} \left(\frac{1}{4}x - \frac{1}{2}, \pm 5\left(y + \frac{3}{4}\right)\right) \\ \qquad\qquad \text{for } (x, y) \in N_0\,, \\ \left(\frac{1}{4}x + \frac{1}{2}, \pm 2\left(y - \frac{3}{4}\right) - \frac{3}{4}\right) \\ \qquad\qquad \text{for } (x, y) \in N_1\,. \end{cases} \tag{5}
$$

Images of N_0 and N_1 under h_d are shown in Fig. 2(b).

From the definition of the deformed Smale's horseshoe it follows that if $\mathbf{x} \in N_1$ then $h_d(\mathbf{x}) \notin N_1$. Hence there are no periodic points of h_d corresponding to sequences containing subsequence $(1, 1)$.

Like in the case of the original Smale's horseshoe one can show that for every periodic point of the deformed horseshoe map the fixed point index of h_d^n is different from zero. An interesting property of the deformed horseshoe map is that the original horseshoe map h_s is embedded in the second iteration of h_d.

2.4. *Theorems on existence of infinitely many periodic orbits*

Let $f : N_0 \cup N_1 \mapsto \mathbb{R}^2$ be a continuous map. The following theorem [Zgliczyński, 1996] states the existence of infinitely many periodic orbits for maps which could be appropriately homotoped with horseshoe map.

Theorem 1. *If $f(N_0)$, $f(N_1) \subset \text{int} P$, horizontal edges of N_0, N_1 are mapped by f outside of $N_0 \cup N_1$ (in such a way that one of the sets $f(N_{0D})$, $f(N_{0U})$ is enclosed in M_+, while the second one is enclosed in M_-, and similarly for horizontal edges of N_1) then for any finite sequence $a_0, a_1, \ldots, a_{n-1} \in \{0, 1\}^n$ there exists a point $\mathbf{x}$ satisfying*

$$
f^i(\mathbf{x}) \in N_{a_i}, \quad \text{for } i = 0, \ldots, n-1 \text{ and } f^n(\mathbf{x}) = \mathbf{x}\,.
$$

The next theorem considers maps with deformed horseshoe embedded. From the set of n-element sequences with elements from the set $\{0, 1\}$ let us choose sequences which do not contain the subsequence $(1, 1)$:

$$
T_n = \{(a_0, \ldots, a_{n-1}) \in \{0, 1\}^n : (a_j, a_{(j+1) \bmod n}) \\ \neq (1, 1) \text{ for } 0 \le j < n\}\,. \tag{6}
$$

From the definition of the deformed horseshoe map it follows that if $\mathbf{x} \in N_1$ then $h_d(\mathbf{x}) \notin N_1$. Hence there are no periodic points of h_d corresponding to sequences containing the subsequence $(1, 1)$. Thus we have to weaken the proposition of Theorem 2.

Theorem 2. *If $f(N_0)$, $f(N_1) \subset \text{int} P$, horizontal edges of N_0, N_1 are mapped by f in such a way that one of the sets $f(N_{0D})$, $f(N_{0U})$ is enclosed in M_+, while the second one is enclosed in M_-, one of the sets $f(N_{1D})$, $f(N_{1U})$ is enclosed in M_-, while the second one is enclosed in $M_0 \cup N_1 \cup M_+$ then for any finite sequence $a = (a_0, a_1, \ldots, a_{n-1}) \in T_n$ there exists a point $\mathbf{x}$ satisfying*

$$
f^i(\mathbf{x}) \in N_{a_i} \quad \text{for } i = 0, \ldots, n-1 \text{ and } f^n(\mathbf{x}) = \mathbf{x}\,. \tag{7}
$$

Proof. As the proof is similar to the proof of Theorem 1 (given in details by Zgliczyński [1996]), we will present only a sketch of it. Let h_d denote the deformed horseshoe map. Let F be a continuous homotopy connecting f with h_d:

$$
F_\lambda(\mathbf{x}) \stackrel{\text{df}}{=} F(\lambda, \mathbf{x}) = (1 - \lambda)f(\mathbf{x}) + \lambda h_d(\mathbf{x})\,.
$$

It is obvious that $F_0 = f$ and $F_1 = h_d$. The homotopy F is constructed in such a way that the assumptions of the theorem are fulfilled for every function F_λ ($\lambda \in [0, 1]$). Let us choose a natural number n and a finite sequence $a = (a_0, a_1, \ldots, a_{n-1}) \in T_n$. Let

$$
N_a^\lambda \stackrel{\text{df}}{=} N_{a_0} \cap F_\lambda^{-1}(N_{a_1}) \cap \cdots \cap F_\lambda^{-(n-1)}(N_{a_{n-1}})\,. \tag{8}
$$

It is clear that there exists a fixed point $\mathbf{x}$ of h_d^n satisfying $h_d^i(\mathbf{x}) \in N_{a_i}$ for $i = 0, 1, \ldots, n-1$.

The proof that for the sequence a there exists $\mathbf{x}$ satisfying (7) consists of several steps.

First we prove that there are no fixed points of the map F_λ^{n+1} on the boundary of the set N_a^λ. From that one can conclude that the fixed point index $I(F_\lambda^{n+1}, N_a^\lambda)$ of the map F_λ^{n+1} with respect to N_a^λ is well defined (compare Definition 1).

From homotopy invariance of the fixed point index (Definition 1, axiom 5) we obtain

$$
I(f^n, N_a^0) = I(F_0^n, N_a^0) = I(F_1^n, N_a^1) = I(h_d^n, N_a^1)\,.
$$

Because the fixed point index of h_d^n with respect to N_a^1 is different from 0 we conclude that $I(f^n, N_a^0)$ is also different from zero, and hence (Remark 1) there exists a point $\mathbf{x}$ satisfying (7). ∎

The above theorem was formulated for special positions of sets N_0 and N_1 on the real plane. But one can easily apply this theorem for different positions changing coordinates appropriately.

In order to use Theorem 2 to prove the existence of infinitely many periodic orbits, one has to show that images of sets N_0, N_1 and their horizontal edges are included in certain subsets of the stripe P. When we use a computer to perform this task one of the most important issues is the computation time. The most time-consuming is checking the first assumption of Theorem 2 (namely $f(N_0)$, $f(N_1) \subset P$). If f is one-to-one, then it is possible to weaken the first assumption using the following intuitively clear lemma:

Lemma 1. *Let f be one-to-one, N_0, N_1, P be defined as above. If $f(\partial N_0)$, $f(\partial N_1) \subset P$ then also $f(N_0)$, $f(N_1) \subset P$.*

Proof. This is an immediate conclusion from Jordan's theorem [Dold, 1980]. ∎

As the condition $f(\partial N_0) \subset P$ can be checked much more quickly than the condition $f(N_0) \subset P$ (∂N_0 is one-dimensional, while N_0 is two-dimensional), computation time can be considerably reduced.

3. Infinitely Many Periodic Orbits for Chua's Circuit

We have applied the method presented in the previous section to the Poincaré map generated by the Chua's circuit [Chua 1993]. Chua's circuit is described by the following state equation:

$$
\begin{aligned}
C_1 \dot{x} &= G(y - x) - g(x), \\
C_2 \dot{y} &= G(x - y) + z, \\
L \dot{z} &= -y - R_0 z,
\end{aligned}
\tag{9a}
$$

where $g(\cdot)$ has a three-segment piecewise-linear characteristic

$$
g(x) = G_b x + 0.5(G_a - G_b)(|x+1| - |x-1|). \tag{9b}
$$

We have used the following parameter values: $C_1 = 1$, $C_2 = 9.3515$, $L = 0.06913$, $R = 0.33065$,
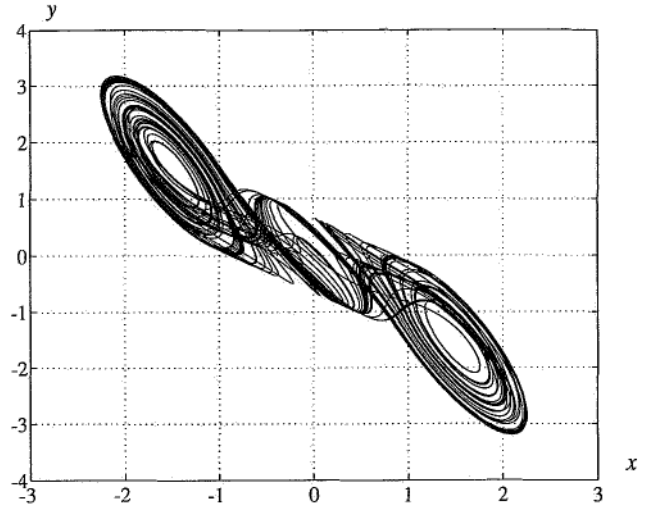

Fig. 3. The double-scroll attractor — computer simulation.

$G_a = -3.4429$, $G_b = -2.1849$, $R_0 = 0.00036$. For this set of parameters the double-scroll chaotic attractor was observed [Chua 1992]. A typical trajectory of the Chua's circuit is shown in Fig. 3.

In our calculations we use the piecewise linearity of the Chua's system. The state space $\mathbb{R}^3$ can be divided into three open regions $U_\pm = \{\mathbf{x} = (x, y, z)^T \in \mathbb{R}^3 : \pm x > 1\}$, $U_0 = \{\mathbf{x} = (x, y, z)^T \in \mathbb{R}^3 : |x| < 1\}$ separated by planes $V_\pm = \{\mathbf{x} \in \mathbb{R}^3 : x = \pm 1\}$. The state equation can be rewritten as:

$$
\dot{\mathbf{x}} = \begin{cases} \mathbf{A}\mathbf{x} & x \in U_0 \\ \mathbf{B}(\mathbf{x} - \mathbf{p}) & \text{if} \quad x \in U_+ \ , \\ \mathbf{B}(\mathbf{x} + \mathbf{p}) & x \in U_- \end{cases}
$$

where $\mathbf{A}$, $\mathbf{B}$ are matrices with real coefficients. In the regions U_0, U_+, U_- the solution of the state equation can be written in the form: $\mathbf{x}(t) = e^{\mathbf{A}t}\mathbf{x}$, $\mathbf{x}(t) = e^{\mathbf{B}t}(\mathbf{x} - \mathbf{p}) + \mathbf{p}$, $\mathbf{x}(t) = e^{\mathbf{B}t}(\mathbf{x} + \mathbf{p}) - \mathbf{p}$ respectively.

In order to use Theorem 2 we define a two-dimensional discrete map arising from the continuous three-dimensional flow. This is a general method which reduces many problems concerning dynamical systems with continuous time to the corresponding problem for dynamical systems with discrete time. This method goes back to Poincaré. He proposed to consider the return map which arises on a transversal surface of codimension 1. In the case of piecewise-linear systems it is natural to choose as a transversal plane one of the planes separating linear regions. Let us choose a transversal section $\Sigma = V_+$. The *Poincaré map* $\mathbf{P} : \Sigma \mapsto \Sigma$ is defined by:

$$
\mathbf{P}(\mathbf{x}) = \mathbf{P}_\Sigma(\mathbf{x}) = \phi_{\tau(\mathbf{x})}(\mathbf{x}), \tag{10}
$$

where $\phi_t(\mathbf{x})$ is a trajectory of the system (9) based at $\mathbf{x}$, $\tau(\mathbf{x})$ is the time needed for the trajectory $\phi_t(\mathbf{x})$ to return to Σ. In general the Poincaré map defined on the whole plane need not be continuous. For Chua's system it is not. We will however find two sets N_0 and N_1 (for the definitions see below) such that $\mathbf{P}$ restricted to these sets is continuous. In order to prove this we will use the following result: If Σ is transversal to the vector field at $\mathbf{x}$ and $\mathbf{P}(\mathbf{x})$ then the existence of a continuous Poincaré map in the neighborhood of $\mathbf{x}$ is ensured [Guckenheimer & Holmes, 1983]. Next we will prove the existence of infinitely many periodic points of the map $\mathbf{P}$ within the set $N_0 \cup N_1$. Periodic points of $\mathbf{P}$ correspond to periodic solutions of Eq. (9).

On the transversal plane Σ we choose eight points

$$A_1 = (-0.1950, -2.6942956550),$$
$$A_2 = (-0.1761, -2.2243882059),$$
$$A_3 = (-0.2376, -2.9659317744),$$
$$A_4 = (-0.2410, -3.2489461290),$$
$$A_5 = (-0.3181, -4.1785885539),$$
$$A_6 = (-0.3315, -4.0981421985),$$
$$A_7 = (-0.3597, -4.4381670543),$$
$$A_8 = (-0.3472, -4.5294652668).$$

lying on two parallel lines: $z = (y \cdot 1.253 - 0.0105) \cdot 9.623$, $z = (y \cdot 1.253 - 0.03565) \cdot 9.623$. Let N_1 be the quadrangle $A_1 A_2 A_3 A_4$, and N_0 be the quadrangle $A_5 A_6 A_7 A_8$. The "horizontal" sides of N_0 and N_1 are defined as $N_{1U} = \overline{A_1 A_2}$, $N_{1D} = \overline{A_3 A_4}$, $N_{0U} = \overline{A_5 A_6}$, $N_{0D} = \overline{A_7 A_8}$ (compare Fig. 4).
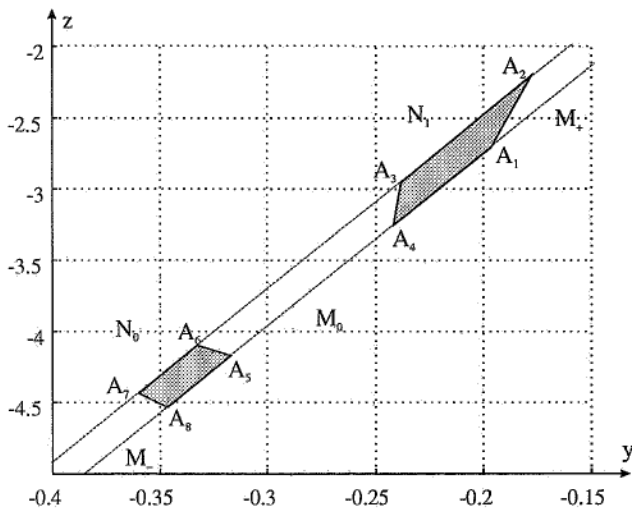

Fig. 4.   Sets N_0, N_1, M_-, M_0 and M_+ on transversal plane.

We have proved that for the Poincaré map associated with the Chua's circuit and for quadrangles N_0 and N_1 defined above, the assumptions of Theorem 2 are fulfilled. Details are given in the following sections.

3.1. *Interval arithmetic*

To use the existence theorems given in Sec. 2 one has to check in every particular case whether the images of edges of sets N_0, N_1 are included in appropriate subsets of the stripe P. To prove this one can use the computer. The considered set is covered by rectangles. Then the image of each one of these rectangles is computed and the condition of whether this image lies appropriately with respect to sets N_0, N_1 is checked. In order to take into account computational errors, we have used interval arithmetic [Alefeld & Herzberger, 1983]. Interval arithmetic is a method of computing intervals containing the true values. A result of a single operation is an interval containing all possible results. For example, the sum of two intervals is an interval containing all possible results of addition, namely $[a, b] + [c, d] \supseteq \{x = x_1 + x_2 : x_1 \in [a, b], x_2 \in [c, d]\}$. During computations we used procedures for interval arithmetic called BIAS (Basic Interval Arithmetic Subroutines) prepared by Olaf Knüppel from Technical University Hamburg-Harburg. We used gnu C++ compiler on Sun SPARC workstation.

In order to check the results we have prepared another package for interval computations. It has been implemented using Borland Pascal and run on PC-486.

To use interval computations for proving mathematical theorems we must make several assumptions. First we assume that all basic interval operations are implemented properly, i.e. for all intervals $[a, b]$, $[c, d]$

$$[a, b] \diamond [c, d] \supseteq \{x = x_1 \diamond x_2 : x_1 \in [a, b], x_2 \in [c, d]\}. \quad (11)$$

where $\diamond$ is any of the following operators: $+, -, \cdot, /$. Usually during preparation of a package for interval computations, one assumes that all digits computed by computer are accurate. The easiest way to compute for example result of multiplication of two intervals $[a, b]$ and $[c, d]$ is to multiply ends of the intervals $a \cdot c$, $a \cdot d$, $b \cdot c$, $b \cdot d$, choose the smallest interval containing all of these four numbers and modify ends of this interval to take into account computer

errors made during multiplication. There are more sophisticated methods requiring only two multiplications. Once we have four basic interval operations we can construct procedures for more complicated functions. During computations we have used functions sin, cos, exp. We also assumed that they are implemented properly, i.e. for every interval $[a, b]$

$$\text{fun}([a, b]) \supseteq \{\text{fun}(x) : x \in [a, b]\}, \qquad (12)$$

where fun is any of the functions sin, cos, exp. This assumption can easily be checked (if we first prove that basic operators are implemented properly) because functions sin, cos, exp are implemented using operators $+, -, \cdot, /$ (usually one uses a truncation of a Taylor series and takes account of errors caused by omitting components of greater order).

3.2. *Existence of an infinite number of periodic orbits*

In computer simulations, we have integrated Eqs. (9) using a fourth-order Runge–Kutta method with time step 0.1. We have observed the deformed horseshoe embedded in the Poincaré map. In Fig. 5 one can see two quadrangles N_0, N_1 and their images under the Poincaré map. The picture is similar to the deformed horseshoe from Fig. 2(b). The next step is to mathematically prove this observation. Using interval computations we were able to prove the following theorem:

Theorem 3. *For all parameter values in a sufficiently small neighborhood of* $(C_1, C_2, L, R, G_a,$
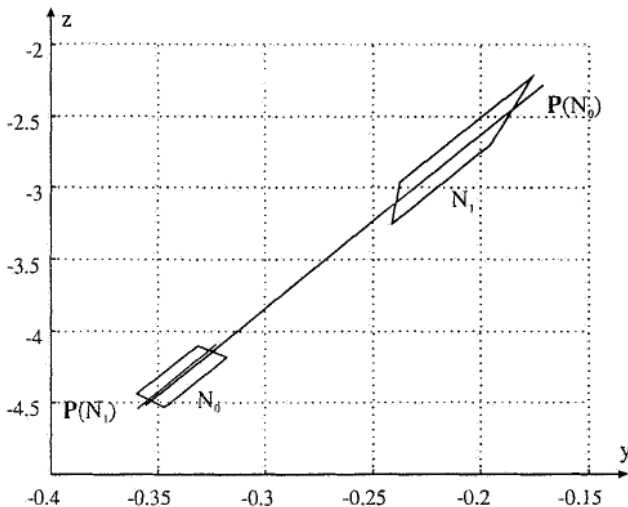
Fig. 5. Sets N_0, N_1 and their images under the Poincaré map — computer simulations.

$G_b, R_0) = (1, 9.3515, 0.06913, 0.33065, -3.4429, -2.1849, 0.00036)$

(1) *There exists a continuous Poincaré map defined on* $N_0 \cup N_1$,
(2) *Images* $\mathbf{P}(N_{0L})$, $\mathbf{P}(N_{0R})$, $\mathbf{P}(N_{1L})$, $\mathbf{P}(N_{1R})$ *of "vertical" edges of quadrangles* N_0, N_1 *lie inside stripe* P,
(3) *Images of "horizontal" edges of* N_0, N_1 *fulfill the following conditions:* $\mathbf{P}(N_{0D}) \subset M_+$, $\mathbf{P}(N_{0U}) \subset M_-$, $\mathbf{P}(N_{1D}) \subset M_-$, $\mathbf{P}(N_{1U}) \subset M_0$.

Proof. The main problem of computer calculations in our case is the computation of the image of a rectangle under Poincaré map. We have developed a procedure carrying out this task. A detailed description of this procedure is given in the appendix. Once this procedure was ready we were able to check the three assumptions.

(1) In the first step we proved that there exists continuous Poincaré map defined on $N_0 \cup N_1$. The set N_0 was covered by 574 890 rectangles. The set N_1 was covered by 451 rectangles. We computed images of these rectangles under the Poincaré map, proving in this way the existence of a continuous Poincaré map.
(2) Vertical edges N_{1L}, N_{1R} were covered by 1501 and 1000 rectangles respectively. N_{0L}, N_{0R} were covered by 7631 and 7969 rectangles. We proved that images of all of these rectangles lie in the stripe P.
(3) Horizontal edges N_{1U}, N_{1D} were covered by 1500 and 298 rectangles respectively. N_{0U}, N_{0D} were covered by 2986 and 30 000 rectangles. We proved that $f(N_{1U})$, $f(N_{1D})$, $f(N_{0U})$, $f(N_{0D})$ are enclosed within the sets P_{1U}, P_{1D}, P_{0U}, P_{0D} shown in Fig. 6.

The greater numbers in the case of N_0 are caused by stronger repelling action for trajectories starting in N_0, especially in the neighborhood of N_{0D}. In this region the unstable eigenvalue of the Jacobian was estimated to be greater than 30 in absolute value, while in the region N_1 both eigenvalues are stable (smaller than 1 in absolute value). ■

Using Theorems 2, 3 and Lemma 1, we obtain the following theorem:

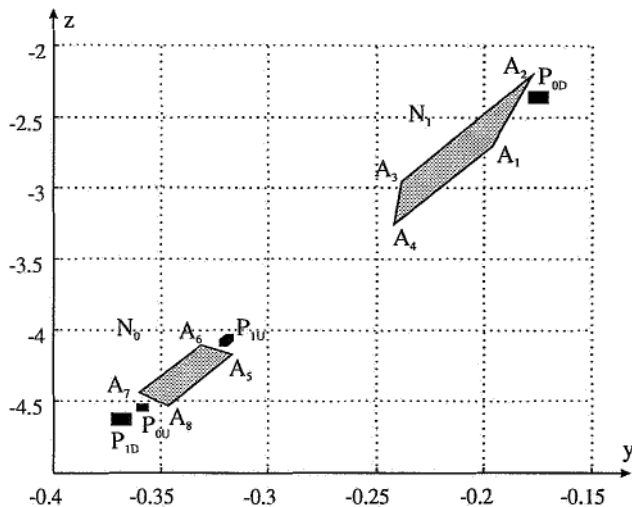**Theorem 4.** *For all parameter values in a sufficiently small neighborhood of* $(C_1, C_2, L, R, G_a,$

Fig. 6. Images of "horizontal" edges of N_0 and N_1 under Poincaré map, $N_{1U} = \overline{A_1 A_2}$, $N_{1D} = \overline{A_3 A_4}$, $N_{0U} = \overline{A_5 A_6}$, $N_{0D} = \overline{A_7 A_8}$, $\mathbf{P}(N_{1U}) \subset P_{1U}$, $\mathbf{P}(N_{1D}) \subset P_{1D}$, $\mathbf{P}(N_{0U}) \subset P_{0U}$, $\mathbf{P}(N_{0D}) \subset P_{0D}$.

$G_b, R_0) = (1, 9.3515, 0.06913, 0.33065, -3.4429, -2.1849, 0.00036)$ *the Poincaré map* $\mathbf{P}$ *has an infinite number of periodic points, strictly speaking for every finite sequence* $a = (a_0, a_1, \ldots, a_{n-1}) \in T_n$ *there exists* $\mathbf{x}$ *such that*

$$\mathbf{P}^i(\mathbf{x}) \in N_{a_i} \quad \text{for } i = 0, \ldots, n-1 \quad \text{and} \quad \mathbf{P}^n(\mathbf{x}) = \mathbf{x}. \tag{13}$$

Proof. From the first part of Theorem 3 it follows that Poincaré map is continuous on $N_0 \cup N_1$. As the left-hand side of the state equation (9) fulfills the global Lipschitz condition, Chua's system has the property of uniqueness of solutions. It follows that the Poincaré map is one-to-one. From the second and third part of Theorem 3, it follows that images of edges of sets N_0 and N_1 under $\mathbf{P}$ are enclosed in the interior of the stripe P. Hence from Lemma 1, $\mathbf{P}(N_0) \subset P$ and $\mathbf{P}(N_1) \subset P$.

From the third part of Theorem 3 it is clear that the images of "horizontal" edges of quadrangles N_0, N_1 lie inside the stripe P outside N_0, N_1. In particular, the following conditions hold: $\mathbf{P}(N_{0D}) \subset M_+$, $\mathbf{P}(N_{0U}) \subset M_-$, $\mathbf{P}(N_{1D}) \subset M_-$, $\mathbf{P}(N_{1U}) \subset M_0$.

Thus the assumptions of Theorem 2 are fulfilled and the proof is completed. ■

4. Topological Entropy

To each discrete dynamical system (X, φ) it is possible to assign a number $h(\varphi)$ known as the entropy of the map φ. Dynamical systems which behave in a non-complex way have zero topological entropy. On the other hand, chaotic systems possess positive topological entropy. In some papers, a chaotic system is by definition a system with positive topological entropy. Hence, it is very important to be able to find or estimate the topological entropy of the system. In this section we prove that topological entropy of the Poincaré map is positive. Later we will also show that the topological entropy of the continuous system defined by Eqs. (9) is positive.

4.1. *Topological entropy of the Poincaré map*

In this section we will estimate from below the topological entropy of the Poincaré map. The notion of topological entropy was introduced by Adler, Konheim and McAndrew [1965]. Let us first recall this definition. Let (X, ϱ) be a compact metric space and α be an open covering of $X : \alpha = \{A_i\}$, $X \subset \bigcup_i A_i$, A_i – open.

Definition 2. If $\alpha = \{A_i\}_{i=1}^n$ and $\beta = \{B_j\}_{j=1}^m$ are open coverings of X, then

$$\alpha \vee \beta = \{A_i \cap B_i, \ i = 1, \ldots, n, \ j = 1, \ldots, m\}$$

is called *product of coverings* α and β.

Definition 3. For open covering α of space X, let $N(\alpha)$ be a number of sets in subcovering with minimum cardinality; subcovering β of covering α is called *minimum*, if every other subcovering of α has not less elements than β. *Topological entropy of covering* α is defined as

$$H_0 = \log N(\alpha).$$

Let $\varphi : X \mapsto X$ be a continuous map.

Definition 4. The limit

$$h(\varphi, \alpha) = \lim_{n \to \infty} \frac{1}{n} H_0(\alpha \vee \varphi^{-1}(\alpha) \vee \cdots \vee \varphi^{-n+1}(\alpha))$$

is called the *topological entropy of* φ *with respect to the covering* α. The number $h(\varphi)$, defined by

$$h(\varphi) = \sup_\alpha h(\varphi, \alpha)$$

is called the *topological entropy of* φ. Supremum is taken over all open coverings α.

Topological entropy $h(\varphi)$ of a discrete dynamical system (X, φ) characterizes "mixing" of points

of X by the map φ. One of important properties of topological entropy is its invariance on topological conjugacy, i.e. if systems (X, φ) and (Y, ψ) are topologically conjugate,[2] then $h(\varphi) = h(\psi)$.

Definition 4 is not convenient for computations. For estimation of topological entropy we will use the equivalent definition based on the notion of (n, ε)-separated sets.

Definition 5. A set $E \subset X$ is called (n, ε)-*separated* if for every two different points x, $y \in E$, there exists $0 \le j < n$ such that $\varrho(\varphi^j(x), \varphi^j(y)) > \varepsilon$.

Bowen [1971] proved the following theorem.

Theorem 5.

$$h(\varphi) = \lim_{\varepsilon \to 0} \limsup_{n \to \infty} \frac{1}{n} \log s_n(\varepsilon), \qquad (14)$$

where

$$s_n(\varepsilon) = \max\{\operatorname{card} E : E \text{ is } (n, \varepsilon)\text{-separated}\}.$$

We will use the above formula to estimate the topological entropy of **P**. Let T_n be defined in (6). Let us denote the cardinality of T_n by P_n. First we will give two lemmas concerning P_n.

Lemma 2. *The formula for P_n reads:*

$$\begin{cases} P_1 = 1, \\ P_2 = 3, \\ P_n = P_{n-1} + P_{n-2} & n \ge 3. \end{cases} \qquad (15)$$

Proof. The proof involves some basic combinatorial operations. ∎

The next lemma gives a nonrecurrence formula for P_n.

Lemma 3.
$$P_n = z_1^n + z_2^n, \qquad (16)$$
where $z_1 = (1 + \sqrt{5})/2$, $z_2 = (1 - \sqrt{5})/2$.

Proof. This lemma can be easily proved with the generating function method. ∎

---

[2]Discrete dynamical systems (X, φ) and (Y, ψ) are *topologically conjugate* if there exists a homeomorphism $h : X \mapsto Y$ such that $h \circ \varphi = \psi \circ h$.

Remark 2. P_n is the number of fixed points of map h_d^n.

Now we can compute the lower bound of topological entropy of the map **P**.

Theorem 6. *Let* **P** *be a Poincaré map defined in* (10). *Then for all parameter values in a sufficiently small neighborhood of* $(C_1, C_2, L, R, G_a, G_b, R_0) = (1, 9.3515, 0.06913, 0.33065, -3.4429, -2.1849, 0.00036)$

$$h(\mathbf{P}) \ge \log \frac{1 + \sqrt{5}}{2}. \qquad (17)$$

Proof. Let us choose $\delta \le \inf_{\mathbf{x} \in N_0, \mathbf{y} \in N_1}\{d(\mathbf{x}, \mathbf{y})\}$. Let us choose a positive integer n, and a positive real $\varepsilon < \delta$. For every sequence $a \in T_n$ we choose $\mathbf{x}_a$ satisfying (7). From Theorem 2 it follows that such $\mathbf{x}_a$ exists. Let us define

$$E_n = \{\mathbf{x}_a\}_{a \in T_n}.$$

We will show that the set E_n is (n, ε)-separated. Let us choose two different points $\mathbf{x}_a$, $\mathbf{x}_b$. If sequences $a, b \in T_n$ are different then there exists $0 \le i < n$ such that $a_i \ne b_i$. From (13) it follows that $\mathbf{P}^i(\mathbf{x}_a) \in N_{a_i}$ and $\mathbf{P}^i(\mathbf{x}_b) \in N_{b_i}$. Because $\varepsilon < \delta \le \inf_{\mathbf{x} \in N_0, \mathbf{y} \in N_1}\{d(\mathbf{x}, \mathbf{y})\}$ then $d(\mathbf{P}^i(\mathbf{x}_a), \mathbf{P}^i(\mathbf{x}_b)) > \varepsilon$ and E_n is (n, ε)-separated. The cardinality of E_n is P_n. Hence $s_n(\varepsilon) \ge P_n$.

$$h(\mathbf{P}) = \lim_{\varepsilon \to 0} \limsup_{n \to \infty} \frac{1}{n} \log s_n(\varepsilon) \ge \limsup_{n \to \infty} \frac{1}{n} \log P_n$$

$$= \lim_{n \to \infty} \frac{1}{n} \log P_n = \lim_{n \to \infty} \log \sqrt[n]{z_1^n + z_2^n}$$

$$= \log z_1 = \log \frac{1 + \sqrt{5}}{2}. \qquad ∎$$

Because $(1 + \sqrt{5})/2 > 1$, we obtain the following corollary.

Corollary 1. *For all parameter values in a sufficiently small neighborhood of* $(C_1, C_2, L, R, G_a, G_b, R_0) = (1, 9.3515, 0.06913, 0.33065, -3.4429, -2.1849, 0.00036)$ *the Poincaré map* **P** *is chaotic in the sense that it has positive topological entropy.*

There are other possibilities to estimate topological entropy using the number of periodic orbits. The most famous result is Bowen's theorem

concerning axiom A diffeomorphisms.[3] Topological entropy of an axiom A diffeomorphism is equal to

$$h(\varphi) = \lim_{n \to \infty} \frac{\log C(\varphi^n)}{n},$$

where $C(\varphi^n)$ denotes the number of fixed points of φ^n [Szlenk, 1984]. Unfortunately we cannot use this theorem in our case due to very restrictive assumptions. It is possible to show that for the Poincaré map $\mathbf{P}$ the decomposition into stable and unstable directions on $N_0 \cup N_1$ does not exist.

The next possibility is to compute the topological entropy of the subshift of finite type on two symbols using its transition matrix. Let $\sigma: \Sigma_2 \mapsto \Sigma_2$ be a full shift defined on a space of infinite sequences with elements from the set $\{0, 1\}$. Let Σ_d be a subset of Σ_2 composed of sequences which does not contain subsequence $(1, 1)$. Σ_d is invariant under shift σ. The subshift of finite type $\sigma|\Sigma_d$ corresponding to the deformed horseshoe map has a transition matrix equal to

$$\mathbf{A} = \begin{pmatrix} 1 & 1 \\ 1 & 0 \end{pmatrix}.$$

Topological entropy of a subshift of finite type with transition matrix $\mathbf{A}$ equals to the logarithm of an eigenvalue λ_1 of $\mathbf{A}$ such that $\lambda_1 \geq |\lambda_j|$ for all eigenvalues of $\mathbf{A}$ [Robinson]. From that we obtain $h(\sigma|\Sigma_d) = (1 + \sqrt{5})/2$. In order to use this result to estimate the topological entropy of the Poincaré map, one has to prove that there exists a semiconjugacy[4] between $\mathbf{P}$ restricted to some invariant set $D \subset N_0 \cup N_1$ and $\sigma|\Sigma_d$, i.e. there exists a continuous surjection $g: D \mapsto \Sigma_d$ such that $g \circ \mathbf{P}|D = \sigma \circ g$. After proving that $\mathbf{P}|D$ and $\sigma|\Sigma_d$ are semiconjugate, the topological entropy $h(\mathbf{P})$ can be estimated from below in the following way: $h(\mathbf{P}) \geq h(\mathbf{P}|D) \geq h(\sigma|\Sigma_d)$ [Robinson, 1995]. This is another proof of Theorem 6.

---

[3]We say that diffeomorphism φ defined on manifold M is an *axiom A diffeomorphism* if the set of nonwandering points $\Omega(\varphi)$ is hiperbolic and periodic points of φ are dense in $\Omega(\varphi)$. A set E is called *hiperbolic* if at every point $x \in E$ there exists a decomposition into stable and unstable directions and this decomposition is continuous. A point x is called *nonwandering* if for every neighborhood U of x and for every $n > 0$ there exists $m > n$ such that $\varphi^m(U) \cap U \neq \emptyset$.

[4]We say that maps $f: X \mapsto X$ and $g: Y \mapsto Y$ are *semiconjugate* if there exist a continuous surjection $k: X \mapsto Y$ such that $k \circ f = g \circ k$. For semiconjugate maps f, g we have the following inequality $h(f) \geq h(g)$.

4.2.   *Topological entropy of the flow*

First we will introduce the definition of the topological entropy for continuous systems [Cornfeld *et al.*, 1982].

Definition 6. A *dynamical system* on X is the triplet (X, T, π), where $T = \mathbb{R}$ (a *continuous* dynamical system or a *flow*) or $T = \mathbb{Z}$ (a *discrete* dynamical system or a *cascade*) and π is a continuous map from the product space $X \times T$ into the space X satisfying the following axioms: $\pi(x, 0) = x$, $\pi(\pi(x, t_1), t_2) = \pi(x, t_1 + t_2)$ for every $x \in X$ and $t_1, t_2 \in T$.

An important class of continuous dynamical systems are systems generated by autonomous ordinary differential equations $\dot{x} = F(x)$ possessing the property of uniqueness of solutions [Guckenheimer & Holmes, 1983]. Chua's circuit is an example of such a system.

The notion of topological entropy can be extended to continuous systems. Let $(X, \mathbb{R}, \pi)$ be a continuous dynamical system.

Definition 7. *Topological entropy* of a flow $(X, \mathbb{R}, \pi)$ is a topological entropy of the map π_1

$$h(\pi) \stackrel{\mathrm{df}}{=} h(\pi_1), \tag{18}$$

where $\pi_t: X \mapsto X$ is defined as $\pi_t(x) \stackrel{\mathrm{df}}{=} \pi(x, t)$.

The following theorem [Cornfeld *et al.*, 1982] states that this definition is natural.

Theorem 7. *Let $(X, \mathbb{R}, \pi)$ be a continuous dynamical system. Then $h(\pi_t) = |t| \cdot h(\pi_1)$.*

Existence of infinitely many periodic orbits of $\mathbf{P}|N_0 \cup N_1$ (or in other words positive entropy of the Poincaré map $\mathbf{P}$) can be used to prove that the topological entropy of the flow is positive.

Theorem 8. *For all parameter values in a sufficiently small neighborhood of $(C_1, C_2, L, R, G_a, G_b, R_0) = (1, 9.3515, 0.06913, 0.33065, -3.4429, -2.1849, 0.00036)$ the topological entropy of the flow π generated by Eqs. (9) is positive*

$$h(\pi) > 0.$$

Proof. Let us choose open neighborhoods N_0', N_1' of sets N_0 and N_1 in the transversal plane Σ in such

a way that $N_0' \cap N_1' = \emptyset$ and Σ is transversal to the flow on the set $N_0' \cup N_1'$. It is possible because Σ is transversal to the flow on N_0 and N_1 and the vector field is continuous.

Let us choose a real number T with $T > \tau(\mathbf{x})$ for every $\mathbf{x} \in N_0 \cup N_1$, where $\tau(\mathbf{x})$ is the time after which the trajectory based at $\mathbf{x}$ returns to the plane Σ. Such finite T exists because $\mathbf{P}$ is defined on the compact set $N_0 \cup N_1$.

Let $N_0(\delta)$ denote the intersection of the neighborhood of the set N_0 with radius δ and region U_+:

$$N_0(\delta) = \{\mathbf{x}: d(\mathbf{x}, \mathbf{y}) < \delta \text{ for some } \mathbf{y} \in N_0\} \cap U_+.$$

Similarly we define $N_1(\delta)$. There exists δ such that trajectories starting from points belonging to $N_0(3\delta)$ intersect Σ first at the point belonging to N_0' and such that trajectories starting from points belonging to $N_1(3\delta)$ intersect Σ first at the point belonging to N_1'. The existence of such positive δ follows from transversality of the flow to the plane Σ on the set $N_0' \cup N_1'$.

Let us denote by M the set of points belonging to trajectories starting from $N_0 \cup N_1$ until they return to the plane Σ

$$M = \{\mathbf{x}: \mathbf{x} = \pi(\mathbf{y}, t) \text{ for some}$$
$$\mathbf{y} \in N_0 \cup N_1 \text{ and } t \in [0, \tau(\mathbf{y})]\}.$$

Let us choose t such that $d(\mathbf{x}, \pi(\mathbf{x}, t)) < \delta$ for every $\mathbf{x} \in M$. The existence of $t > 0$ follows from compactness of M. Let N be a natural number greater than T/t. Let E_n be as in (4.1), with the set of fixed points of $\mathbf{P}^n$ indexed by sequences $a \in T_n$. We will show that E_n is (Nn, δ)-separated with respect to the map $\pi_t: \mathbb{R}^3 \mapsto \mathbb{R}^3$ defined by $\pi_t(\mathbf{x}) = \pi(\mathbf{x}, t)$, i.e. for any two different points $\mathbf{x}_a, \mathbf{x}_b \in E_n$, there exists $0 \leq j < nN$ such that $d(\pi(\mathbf{x}_a, jt), \pi(\mathbf{x}_b, jt)) > \delta$.

Suppose that sequences a and b are different and that for $\mathbf{x}_a, \mathbf{x}_b \in E_n$, the condition

$$d(\pi(\mathbf{x}_a, jt), \pi(\mathbf{x}_b, jt)) \leq \delta$$

holds for every natural $j \in \{0, Nn - 1\}$. We will show that sequences a and b are equal.

Let $i \in \{0, n\}$ be the smallest integer number with $a_i \neq b_i$. Assume that $a_i = 0$. Becasue π_t moves points not more than δ, then before the intersection of the trajectory with the set N_0, a discrete trajectory must fall into the set $N_0(2\delta)\backslash N_0(\delta)$. Hence there exists $p \in \{0, Nn - 1\}$ such that $\pi(\mathbf{x}_a, pt) \in N_0(2\delta)\backslash N_0(\delta)$. From the assumption about the

points $\mathbf{x}_a, \mathbf{x}_b$ we have $\pi(\mathbf{x}_b, pt) \in N_0(3\delta)$. But a trajectory starting from $N_0(3\delta)$ must intersect Σ and the intersection point belongs to N_0, and what follows symbol b_i for $\mathbf{x}_b$ is equal to a_i. For the case $a_i = 1$ the proof is similar.

This is a contradiction and hence E_n is (Nn, δ)-separated. It follows that $s_{Nn}(\delta) \geq \text{card } E_n$. Thus

$$h(\varphi_t) = \lim_{\delta \to 0} \limsup_{n \to \infty} \frac{1}{n} \log s_n(\delta)$$

$$\geq \lim_{\delta \to 0} \limsup_{n \to \infty} \frac{1}{Nn} \log s_{Nn}(\delta)$$

$$\geq \lim_{n \to \infty} \frac{1}{Nn} \log \text{card} E_n = \frac{1}{N} \lim_{n \to \infty} \frac{1}{n} \log P_n$$

$$= \frac{1}{N} \log \frac{1 + \sqrt{5}}{2}.$$

From Theorem 7 we obtain the estimation of the topological entropy of the flow:

$$h(\pi) = h(\pi_1) = \frac{1}{t} h(\pi_t) \geq \frac{1}{Nt} \log \frac{1 + \sqrt{5}}{2} > 0. \quad \blacksquare$$

The proof presented above has the advantage that no advanced results are involved. But the above theorem can also be proved in another way using the relationship between topological and measure-theoretic entropies.

Topological entropy of a continuous map f is the supremum of measure-theoretic entropies over measures ergodic with respect to f. This result was conjectured by Adler *et al.* [1965] and proved by Goodwyn, Dinaburg and Goodman. Let ϱ be an invariant probability measure of a continuous time dynamical system and let σ be the probability measure on the transversal plane Σ invariant under the Poincaré map $\mathbf{P}$ and corresponding to ϱ. Let $h(\varrho)$ denote the measure-theoretic entropy of the flow with respect to ϱ and $h(\sigma)$ denote the measure-theoretic entropy of $\mathbf{P}$ with respect to σ. Then we have the following Abramov's formula (compare for example [Eckmann & Ruelle, 1985]):

$$h(\varrho) = \frac{h(\sigma)}{\langle \tau \rangle_\sigma}, \tag{19}$$

where $\langle \tau \rangle_\sigma$ is the average time between two crossings of the section Σ, computed with respect to the probability measure σ. As the topological entropy of $\mathbf{P}$ is positive, there exists a measure σ on Σ such that $h(\sigma) > 0$. In our case, the return time on

$N_0 \cup N_1$ is bounded, hence the average return time is finite and $h(\varrho)$ is also greater than zero. And what follows the topological entropy of the flow is positive as it not less than any measure-theoretic entropy.

5. Periodic Orbits — Simulation Results

Now we address the problem how the number of all periodic orbits of the Poincaré map $\mathbf{P}$ is related to the number of periodic orbits, existence of which was proved before. Results presented in this section are obtained from numerical experiments, hence they are not proved rigorously.

In Sec. 3 we proved (compare Theorem 4) that for every sequence $a = (a_0, a_1, \ldots, a_{n-1}) \in T_n$ there exists a periodic point $\mathbf{x}$ of $\mathbf{P}$ trajectory of which follows this sequence. The number $C(n)$ of fixed points of $\mathbf{P}^n$ existence of which is guaranteed by Theorem 4 grows with n according to Eqs. (15) and (16). Let us denote by $O(n)$ the number of different period-n orbits, composed of these fixed points. $O(n)$ is much smaller than $C(n)$ as several fixed points of $\mathbf{P}^n$ correspond to the same periodic orbit and there are some fixed points of $\mathbf{P}^n$ with period smaller than n. In Table 1 we summarize the values of $O(n)$ and $C(n)$ for n smaller than 11. For example, for $n = 2$ there is only one period-2 orbit of $\mathbf{P}$ corresponding to the sequence $(0,1)$ and there are three fixed points of $\mathbf{P}^2$ with sequences $(0,0)$, $(0,1)$ and $(1,0)$.

In order to find other periodic orbits, we used a heurestic identification procedure based on time series obtained by numerical integration of the system. The trajectory of the Poincaré map consisting of 200 000 points was saved. For this task the Runge–Kutta integration algorithm with time step 0.1 was used. For the identification of periodic orbits we used the method introduced by Lathrop & Kostelich [1989] and its modifications (compare Ogorzałek & Galias [1993]). In Fig. 7, on the left side we show some of the periodic orbits found. On the right side we present corresponding periodic orbits of the continuous system. We use the following notation: by $\gamma_{m,n}$ we denote periodic orbit with m and n scrolls around the points P_+ and P_- respectively, where P_+ and P_- are symmetric equilibria of the Chua's system. The existence of the orbits (a), (b) and (c) is guaranteed by Theorem 4. These are all of the periodic orbits with period less than four, which exist according to Theorem 4 (compare

Table 1). Apart from these orbits we have found many other periodic orbits. Some of them are shown in Figs. 7(d)–7(h). These orbits are not fully enclosed in the set $N_0 \cup N_1$, so Theorem 4 does not say anything about them. All of these orbits have period 2. Orbits (d), (e) are enclosed within the right part of the attractor, and have three and four scrolls around P_+. Note that also orbit (c) has three scrolls around P_+, but orbits (c) and (d) are different, the first one is period-3 orbit and is enclosed in $N_0 \cup N_1$ while the second is period-2 orbit lying outside of $N_0 \cup N_1$. The last three orbits (f), (g) and (h) visit both sides of the attractor. Apart from the periodic orbits shown we have found several other periodic orbits. There are many low period orbits of $\mathbf{P}$ with corresponding orbits of continuous systems with many scrolls in the second part of the double-scroll attractor.

The double scroll attractor is composed of two parts symmetric with respect to the origin. Trajectories starting from $N_0 \cup N_1$ return to the transversal plane Σ without entering the second part of the attractor. Hence it is not possible to explain the whole dynamics of the double scroll attractor by

Table 1. $O(n)$ — the number of different periodic orbits of period n, $C(n)$ — the number of fixed points of $\mathbf{P}^n$.

n	$O(n)$	$C(n)$	Sequences
1	1	1	(0)
2	1	3	$(0,1)$
3	1	4	$(0,0,1)$
4	1	7	$(0,0,0,1)$
5	2	11	$(0,0,0,0,1)$
			$(0,1,0,0,1)$
6	2	18	$(0,0,0,0,0,1)$
			$(0,1,0,0,0,1)$
7	4	29	$(0,0,0,0,0,0,1)$
			$(0,1,0,0,0,0,1)$
			$(0,0,1,0,0,0,1)$
			$(0,0,1,0,1,0,1)$
8	5	47	$(0,0,0,0,0,0,0,1)$
			$(0,1,0,0,0,0,0,1)$
			$(0,0,1,0,0,0,0,1)$
			$(0,1,0,1,0,0,0,1)$
			$(0,1,0,0,1,0,0,1)$
9	8	76	
10	11	123	

investigation of the Poincaré map on the set $N_0 \cup N_1$. Deformed horseshoe maps embedded within the Poincaré map were also observed for parameter values for which the Rössler-type attractor exists (although we did not prove this fact rigorously). Moreover we have also found periodic orbits [compare Figs. 7(d) and 7(e)] which always stayed in one part of the attractor (so they belong to one Rössler-type attractor), whose existence does not follow from Theorem 4. This is an indication that the Poincaré map of the Rössler-type attractor has more complex dynamics than the deformed horseshoe map. The double-scroll attractor is born by the collision of two symmetric Rössler-type
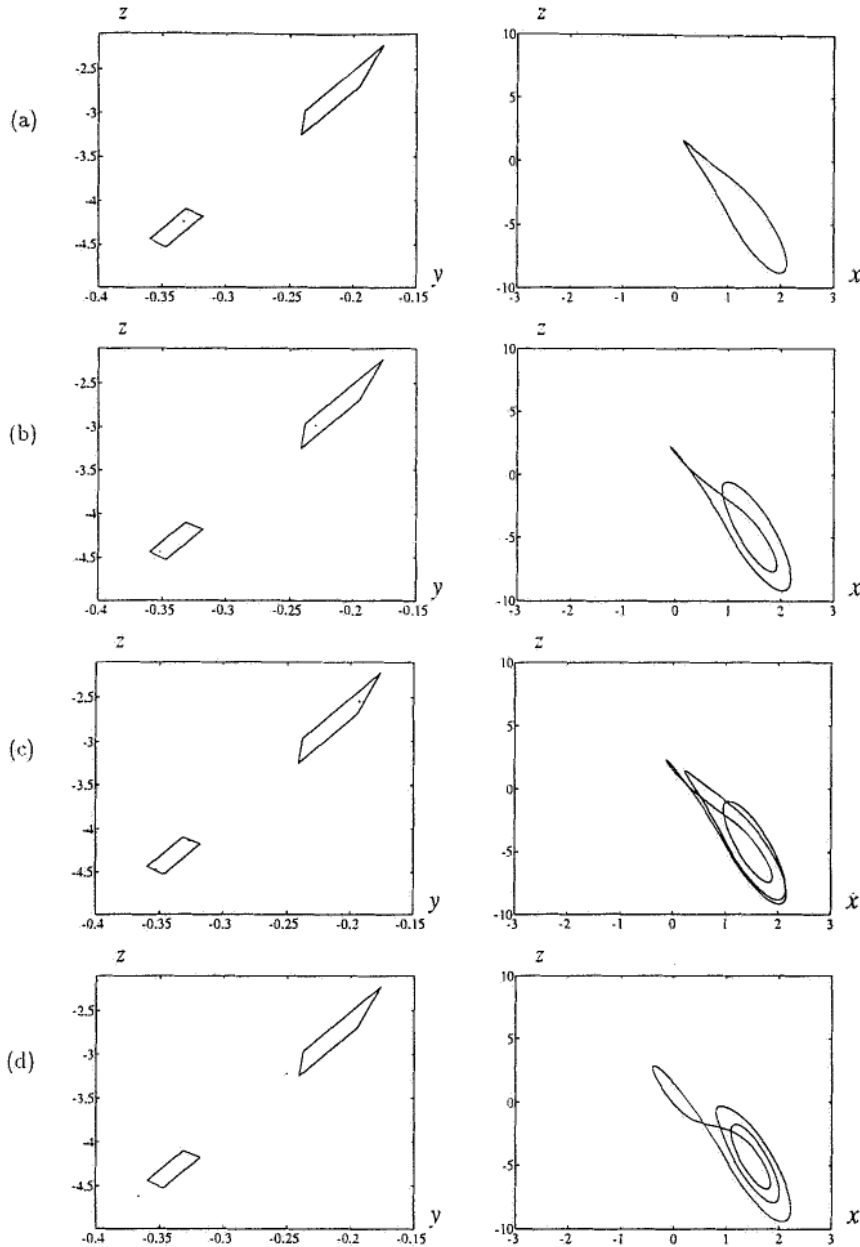
Fig. 7. Periodic orbits of the Poincaré map and corresponding periodic orbits of the continuous system, by $\gamma_{m,n}$ we denote periodic orbit with m scrolls around P_+ and n scrolls around P_-, (a) fixed point with the sequence (0) — $\gamma_{1,0}$ periodic orbit of the continuous system, (b) periodic orbit with the sequence $(0,1)$ — $\gamma_{2,0}$ periodic orbit of the continuous system, (c) periodic orbit with the sequence $(0,0,1)$ — $\gamma_{3,0}$ periodic orbit, (d) period-2 orbit lying outside of $N_0 \cup N_1$ — $\gamma_{3,0}$ periodic orbit. Some of the period-2 orbits of the Poincaré map and corresponding periodic orbits of the continuous system, (e) $\gamma_{4,0}$, (f) $\gamma_{2,2}$ symmetric orbit, (g) $\gamma_{3,3}$ symmetric orbit, (h) $\gamma_{3,3}$ unsymmetric orbit.
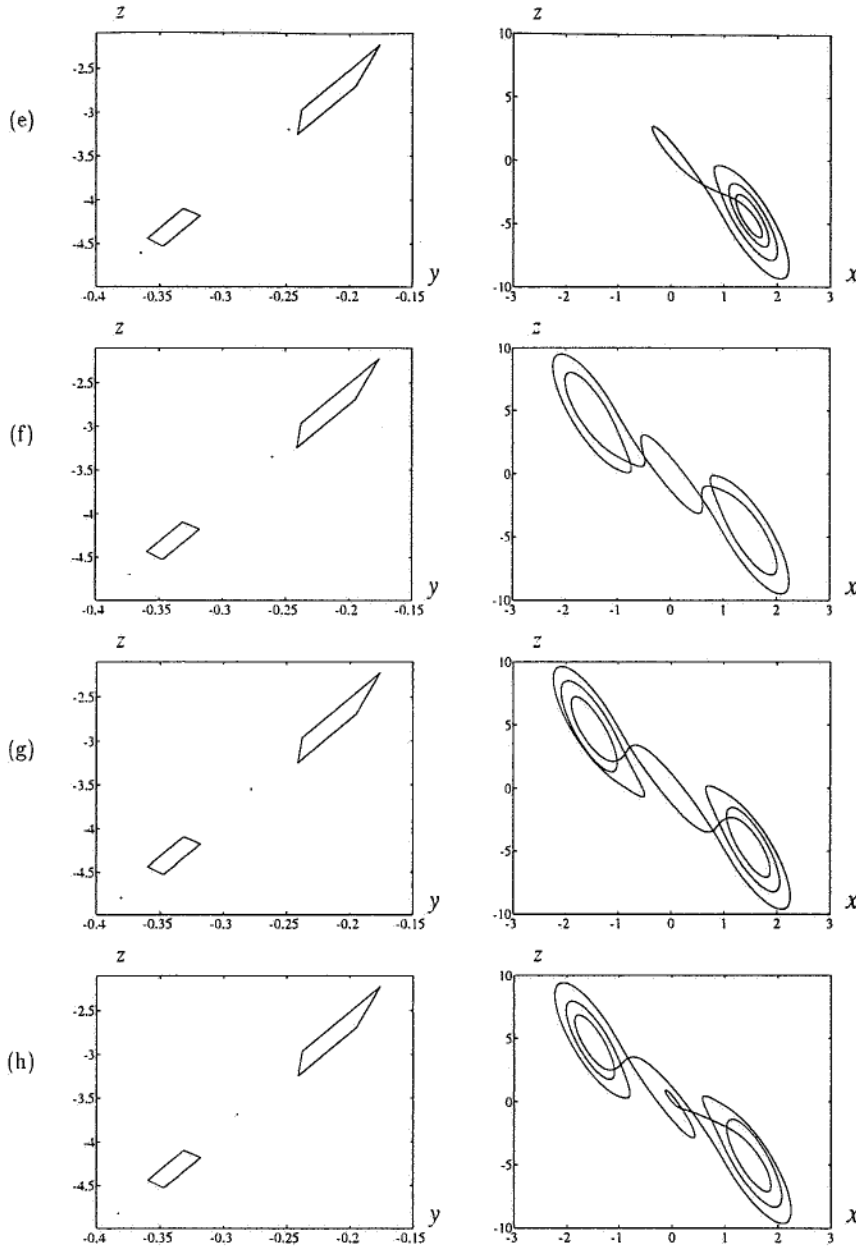
Fig. 7.   (*Continued*)

attractors, and hence its dynamics is much more complex than the one on the Rössler-type attractor.

From the above considerations it follows that the dynamics of the Poincaré map is much more complicated that the one of the deformed horseshoe. The topological entropy of the Poincaré map is then probably greater than the estimation obtained with periodic orbits of the deformed horseshoe map [compare Eq. (17)]. There are some regions in the Σ plane with much greater numbers of periodic orbits for given n than in the region

$N_0 \cup N_1$. Trajectories which enter the second region sometimes stay in this region for a long time before coming back to the transversal plane increasing the topological entropy of $\mathbf{P}$.

We made a simulation in order to compare how sets N_0 and N_1 are related to the chaotic trajectory obtained in computer simulations. The results are shown in Fig. 8. Chaotic trajectory intersects both of the sets N_0 and N_1, creating very complicated sequence of symbols. This is another confirmation that the behavior of Chua's circuit observed in experiments is complex.
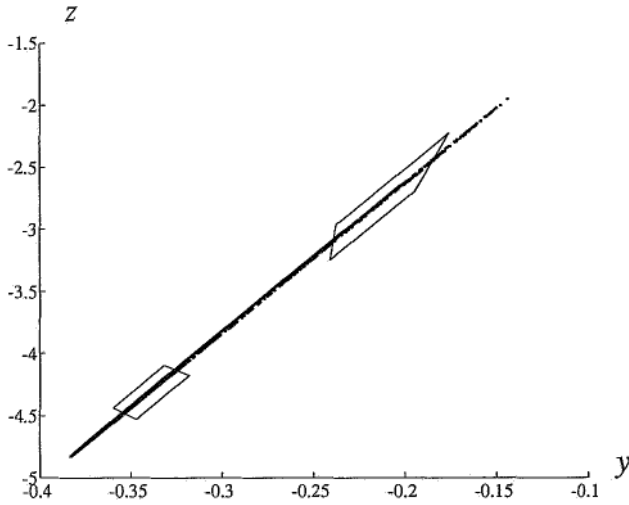
Fig. 8. Quadrangles N_0, N_1 and system's trajectory.

6. Conclusions

The technique for proving the existence of infinitely many periodic orbits for maps with deformed horseshoe embedded was presented. This technique is based on the construction of an appropriate homotopy between the considered map and the deformed horseshoe map, for which dynamical behavior is much better known. It provides a strong description of the dynamics of the considered system (its dynamics is at least as complicated as for the deformed horseshoe map). This technique was successfully applied to Chua's circuit. Using interval arithmetic we carried out a computer-assisted proof of the existence of infinitely many periodic orbits for Chua's circuit. This result was then used to estimate from below the topological entropy of the system. We proved that it is positive. Finally we proved that the topological entropy of the flow generated by equations describing Chua's circuit is positive.

An alternative method is based on Shilnikov's theorem [Tresser, 1984]. When using this theorem, the only thing one has to prove is the existence of homoclinic orbits and some relations between eigenvalues of the system at the homoclinic point. Then from Shilnikov's theorem it follows that there exists a Smale's horseshoe and an infinite number of periodic orbits in the neighborhood of this homoclinic orbit. The problem is that usually we are not able to prove the existence of homoclinic orbits for a given set of parameters. Usually we can only find an interval containing a point for which there exists a homoclinic orbit. In the paper [Chua

et al., 1986], the existence of homoclinic orbit for Chua's system was proved for some unknown parameter values. In contrast with methods based on the Shilnikov's theorem, by using the method presented in this paper one can show the existence of infinitely many periodic orbits and the semiconjugacy with a shift of finite type for a given set of parameters. Another advantage of this method is that it can be applied practically without any modifications for different (not piecewise-linear) types of nonlinearities. In fact it can be used for any differential equations, for which the numerical integration gives a Poincaré map similar to that of the deformed horseshoe. In that case however, one has to take into account errors caused by numerical integration [Galias & Zgliczyński, 1996]. It is also possible to generalize the method for the case of greater number of quadrangles and for different deformations of the horseshoe map [Zgliczyński, 1996].

The methods for proving the existence of horseshoe maps or positivity of topological entropy are sometimes understood as methods for proving chaos. But most often the system is called chaotic (there are many definitions in the literature) if there exists a chaotic attractor for that system (for the definition of chaotic attractor, see for example [Guckenheimer & Holmes, 1983]). The method presented in this paper and also methods based on Shilnikov's theorem are not able to prove the existence of a chaotic attractor. The existence on an infinite number of periodic orbits and positivity of topological entropy are conditions weaker than the existence of a chaotic attractor. It is possible that we do not observe chaotic trajectories although topological entropy is positive because trajectories are repelled from the region with positive entropy. Hence this type of proof of existence of chaos should be considered as incomplete.

Acknowledgments

References

Adler, R., Konheim, A. & McAndrew, M. [1965] "Topological entropy," *Trans. Am. Math. Soc.* **114**, 309–319.

Alefeld, G. & Herzberger, J. [1983] *Introduction to Interval Computations* (Academic Press, New York).

Bilingsley, P. [1965] *Ergodic Theory and Information* (Wiley, New York).

Bowen, R. [1971] "Periodic points and measures for Axiom A diffeomorphisms," *Trans. Am. Math. Soc.* **154**, 377–397.

Chua, L. O., Komuro, M. & Matsumoto, T. [1986] "The double scroll family," *IEEE Trans. Circ. Syst.* **33**, 1037–1118.

Chua, L. O. [1992] "A zoo of strange attractors from the canonical Chua's circuit," Memorandum No. UCB/ERL M92/87, College of Eng., Univ. of California, Berkeley.

Chua, L. O. [1993] "Global unfolding of Chua's circuit," *IEICE Trans. Fundamentals* **E76-A**(5), 704–734.

Cornfeld, I. P, Fomin, S. V. & Sinai, Ya. G. [1982] *Ergodic Theory* (Springer Verlag, New York, Heidelberg Berlin).

Dold, A. [1980] *Lectures on Algebraic Topology* (Springer Verlag, Berlin).

Eckmann, J. P., Ruelle, D. [1985] "Ergodic theory of chaos and strange attractors," *Rev. Mod. Phys.* **57**(3) Part I, 617–656.

Galias, Z. & Zgliczyński, P. [1996] "Proof of chaos for Lorenz system," *Proc. Interval'96* (Würzburg, Germany), pp. 40–42.

Granas, A. [1972] "The Leray–Schauder index and the fixed point theory for arbitrary ANR's," *Bull. Soc. Math., France* **100**, 209–228.

Guckenheimer, J. & Holmes, P. [1983] *Nonlinear Oscillations, Dynamical Systems, and Bifurcations of Vector Fields* (Springer Verlag, New York).

Lathrop, D. P. & Kostelich, E. J. [1989] "Characterization of an experimental strange attractor by periodic orbits", *Phys. Rev.* **A40**(7), 4028–4031.

Mischaikow, K. & Mrozek, M. [1995] "Chaos in the Lorenz equations: A computer assisted proof," *Bull. Amer. Math. Soc.*, **32**(1), 66–72.

Ogorzałek, M. J. & Galias, Z. [1993] "Characterization of chaos in Chua's oscillator in terms of unstable periodic orbits," *J. Circ. Syst. Comput.* **3**(2), 411–429.

Robinson, C. [1995] *Dynamical Systems: Stability, Symbolic Dynamics, and Chaos* (CRC Press, USA).

Szlenk, W. [1984] *An Introduction to the Theory of Smooth Dynamical Systems* (PWN, John Wiley and Sons, Warszawa, Chichester).

Tresser, C. [1984] "About some theorems by L. P. Šil'nikov," *Ann. Inst. Henri Poincaré* **40**(4), 441–461.

Zgliczyński, P. [1996] "Fixed point index for iterations of maps, topological horseshoe and chaos," to appear in *Topological Methods in Nonlinear Analysis*, J. of the Juliusz Schauder Center, Poland.

Appendix
Details of Computer Calculations

Now we will describe in detail a procedure for the computation of an image of a rectangle under the Poincaré map. An input value is a rectangle, an image of which we want to obtain. The procedure finds a rectangle containing an image of an input rectangle. All computational errors are taken into account and cause an increase of the output rectangle. In order to avoid misunderstanding we will denote intervals (and also vectors and matrices of intervals) by adding a "hat" ^ over them. If $\hat{x}$ is an interval then by $\inf(\hat{x})$ and $\sup(\hat{x})$ we will denote the lower and upper end of $\hat{x}$. To simplify notation, a rectangle $[y_1, y_2] \times [z_1, z_2]$ contained in the transversal plane Σ will be denoted by $\hat{\mathbf{x}} = (1, [y_1, y_2], [z_1, z_2])^T$.

Preliminary calculations

First we have to calculate several values necessary for further computations.

(1) Initialization of matrices $\hat{\mathbf{A}}_0$, $\hat{\mathbf{A}}_1$ and vectors $\hat{\mathbf{v}}_0$, $\hat{\mathbf{v}}_1$.

$$\hat{\mathbf{A}}_0 = \begin{pmatrix} -1/(\hat{R}\hat{C}_1) - \hat{G}_a/\hat{C}_1 & 1/(\hat{R}\hat{C}_1) & 0 \\ 1/(\hat{R}\hat{C}_2) & -1/(\hat{R}\hat{C}_2) & 1/\hat{C}_2 \\ 0 & -1/\hat{L} & -\hat{R}_0/\hat{L} \end{pmatrix}, \quad \hat{\mathbf{v}}_0 = \begin{pmatrix} 0 \\ 0 \\ 0 \end{pmatrix}, \qquad \text{(A.1a)}$$

$$\hat{\mathbf{A}}_1 = \begin{pmatrix} -1/(\hat{R}\hat{C}_1) - \hat{G}_b/\hat{C}_1 & 1/(\hat{R}\hat{C}_1) & 0 \\ 1/(\hat{R}\hat{C}_2) & -1/(\hat{R}\hat{C}_2) & 1/\hat{C}_2 \\ 0 & -1/\hat{L} & -\hat{R}_0/\hat{L} \end{pmatrix}, \quad \hat{\mathbf{v}}_1 = \begin{pmatrix} -(\hat{G}_a - \hat{G}_b)/\hat{C}_1 \\ 0 \\ 0 \end{pmatrix}, \qquad \text{(A.1b)}$$

where, for example, $\hat{R}$ is an interval containing true value of R.

(2) Computation of coefficients of characteristic equations of matrices $\hat{\mathbf{A}}_0$, $\hat{\mathbf{A}}_1$.

(3) Computation of roots of characteristic equations. Each of the matrices $\hat{\mathbf{A}}_0$, $\hat{\mathbf{A}}_1$ possesses one real and two complex eigenvalues. Let us assume that the characteristic equation is of the form

$$\lambda^3 + a_3\lambda^2 + a_2\lambda + a_1 = 0. \quad (A.2)$$

Computation of roots consists of two steps. First we find the real root by the modified bisection method and then we find complex roots using the real root previously found.

- Computation of the real root $\hat{\lambda}$. Let us denote

$$\hat{f}(\lambda) := \lambda^3 + \hat{a}_3\lambda^2 + \hat{a}_2\lambda + \hat{a}_1,$$

where λ is a real number, and $\hat{a}_i$ are intervals containing appropriate coefficients of the characteristic equation (A.2). $\hat{f}(\lambda)$ is an interval because it is a result of computations on intervals. The interval $\hat{\lambda} = [\lambda_1, \lambda_2]$ containing the real root can be found by the procedure presented below. The real number ε_0, defines accuracy of computations (for smaller ε_0, the length of the interval containing λ is smaller and the computation time is longer).

```
begin
  {finding λ₁ such that f̂(λ₁) ⊂ (−∞, 0)}
  λ₁ = −1;
  while sup(f̂(λ₁)) ≥ 0 do λ₁ = 2 * λ₁;
  {finding λ₂ such that f̂(λ₂) ⊂ (0, ∞)}
  λ₂ = 1;
  while inf(f̂(λ₂)) ≤ 0 do λ₂ = 2 * λ₂;
  {Searching for maximum λ₁ such that
      f̂(λ₁) ⊂ (−∞, 0)}
  λ_min = λ₁;
  λ_max = λ₂;
  while (λ_max − λ_min) > ε₀ do begin
    λ_med = (λ_max + λ_min)/2;
    if (sup(f̂(λ_med)) < 0)
    then λ_min = λ_med
    else λ_max = λ_med;
  end;
  λ₁ = λ_min;
  {Searching for minimum λ₂ such that
      f̂(λ₂) ⊂ (0, ∞)}
  λ_min = λ₁;
  λ_max = λ₂;
  while (λ_max − λ_min) > ε₀ do begin
    λ_med = (λ_max + λ_min)/2;
    if (inf(f̂(λ_med)) > 0)
    then λ_max = λ_med
```

```
    else λ_min = λ_med;
  end;
  λ₂ = λ_max;
  λ̂ = [λ₁, λ₂];
end;
```

- Computation of the complex roots $\hat{\alpha} \pm i\hat{\beta}$:

$$\hat{\alpha} = -(\hat{a}_3 + \hat{\lambda})/2,$$

$$\hat{\beta} = \sqrt{-(\hat{a}_3 + \hat{\lambda})^2 + 4(\hat{a}_2 + \hat{\lambda}(\hat{a}_3 + \hat{\lambda}))}. \quad (A.3)$$

(4) Computation of inverse matrices $\hat{\mathbf{A}}_0^{-1}$, $\hat{\mathbf{A}}_1^{-1}$

$$(\hat{\mathbf{A}}^{-1})_{i,j} = (-1)^{i+j}\hat{\mathbf{M}}_{i,j}/\det\hat{\mathbf{A}}.$$

(5) Computation of the fixed points: $\hat{\mathbf{p}}_0 = \hat{\mathbf{A}}_0^{-1}\hat{\mathbf{v}}_0$, $\hat{\mathbf{p}}_1 = \hat{\mathbf{A}}_1^{-1}\hat{\mathbf{v}}_1$.

(6) Computation of eigenvectors of $\hat{\mathbf{A}}_0$, $\hat{\mathbf{A}}_1$. Let $\hat{\mathbf{A}}$ be a matrix with eigenvalues $\hat{\lambda}$, $\hat{\alpha} \pm i\hat{\beta}$. We are searching for column eigenvectors $\hat{\mathbf{x}}_1$, $\hat{\mathbf{x}}_2$, $\hat{\mathbf{x}}_3$ fulfilling the following matrix equation:

$$\hat{\mathbf{A}}(\hat{\mathbf{x}}_1\,\hat{\mathbf{x}}_2\,\hat{\mathbf{x}}_3) = (\hat{\mathbf{x}}_1\,\hat{\mathbf{x}}_2\,\hat{\mathbf{x}}_3)\begin{pmatrix} \hat{\lambda} & 0 & 0 \\ 0 & \hat{\alpha} & -\hat{\beta} \\ 0 & \hat{\beta} & \hat{\alpha} \end{pmatrix}.$$

The eigenvector $\hat{\mathbf{x}}_1$ satisfies $\hat{\mathbf{A}}\hat{\mathbf{x}}_1 = \hat{\lambda}\hat{\mathbf{x}}_1$, while eigenvectors $\hat{\mathbf{x}}_2$ and $\hat{\mathbf{x}}_3$ satisfy the following set of equations: $\hat{\mathbf{A}}\hat{\mathbf{x}}_2 = \hat{\alpha}\hat{\mathbf{x}}_2 + \hat{\beta}\hat{\mathbf{x}}_3$, $\hat{\mathbf{A}}\hat{\mathbf{x}}_3 = -\hat{\beta}\hat{\mathbf{x}}_2 + \hat{\alpha}\hat{\mathbf{x}}_3$. The eigenvectors can be found in the following way:

- computation of the eigenvector $\hat{\mathbf{x}}_1$ from the equation $\hat{\mathbf{A}}\hat{\mathbf{x}}_1 = \hat{\lambda}\hat{\mathbf{x}}_1$.
- computation of the eigenvector $\hat{\mathbf{x}}_2$ from the equation $(\hat{\mathbf{A}} - \hat{\alpha}\mathbf{I})^2\hat{\mathbf{x}}_2 = -\hat{\beta}^2\hat{\mathbf{x}}_2$
- computation of $\hat{\mathbf{x}}_3 := -\hat{\beta}(\hat{\mathbf{A}} - \hat{\alpha}\mathbf{I})^{-1}\hat{\mathbf{x}}_2$,
- creation of the matrix $\hat{\mathbf{E}} := (\hat{\mathbf{x}}_1\,\hat{\mathbf{x}}_2\,\hat{\mathbf{x}}_3)$.

(7) Computation of inverse matrices $\hat{\mathbf{E}}_0^{-1}$, $\hat{\mathbf{E}}_1^{-1}$.

Computation of $e^{\hat{\mathbf{A}}\hat{t}}$

Matrix $\hat{\mathbf{A}}$ with eigenvalues $\hat{\lambda}$, $\hat{\alpha} \pm i\hat{\beta}$ can be expressed as

$$\hat{\mathbf{A}} = \hat{\mathbf{E}}\begin{pmatrix} \hat{\lambda} & 0 & 0 \\ 0 & \hat{\alpha} & -\hat{\beta} \\ 0 & \hat{\beta} & \hat{\alpha} \end{pmatrix}\hat{\mathbf{E}}^{-1}, \quad (A.4)$$

where $\hat{\mathbf{E}}$ is a matrix of eigenvectors. Hence

$$e^{\hat{\mathbf{A}}\hat{t}} = \hat{\mathbf{E}} \begin{pmatrix} e^{\hat{\lambda}\hat{t}} & 0 & 0 \\ 0 & e^{\hat{\alpha}\hat{t}}\cos\hat{\beta}\hat{t} & -e^{\hat{\alpha}\hat{t}}\sin\hat{\beta}\hat{t} \\ 0 & e^{\hat{\alpha}\hat{t}}\sin\hat{\beta}\hat{t} & e^{\hat{\alpha}\hat{t}}\cos\hat{\beta}\hat{t} \end{pmatrix} \hat{\mathbf{E}}^{-1}.$$

$$(A.5)$$

Computation of an image of a point after time $\hat{t}$

In the linear regions, the state equation has the form $\dot{\mathbf{x}} = \mathbf{A}_i(\mathbf{x} - \mathbf{p}_i)$. Hence the image of a rectangle $\hat{\mathbf{x}}$ after time $\hat{t}$ can be computed using the following formula:

$$\hat{\varphi}(\hat{\mathbf{x}}, \hat{t}) = e^{\hat{\mathbf{A}}_i \hat{t}}(\hat{\mathbf{x}} - \hat{\mathbf{p}}_i) + \hat{\mathbf{p}}_i. \qquad (A.6)$$

The above formula is true under the assumption that the trajectory stays in one of the linear regions U_0, U_+ for the time $\hat{t}$.

Computation of the return time

Computation of the return time is the most complicated and time-consuming part of the procedure for the evaluation of $\mathbf{P}$. It will be described for the case of a trajectory starting and returning to V_+ after passing through the region U_+. The procedure in the second case (passing through U_0) is similar. Let us assume that $\hat{\mathbf{x}}$ is a rectangle enclosed in the plane V_+. The procedure for the computation of the return time consists of several steps.

(1) Find t_1 such that the part of the trajectory $\varphi(\hat{\mathbf{x}}, (0, t_1])$ is enclosed in U_+. Computation of $\hat{\varphi}(\hat{\mathbf{x}}, [0, t_1])$ cannot give the required results. Because interval arithmetic takes into account computer error, then the set $\hat{\varphi}(\hat{\mathbf{x}}, [0, t_1])$ computed using Eq. (A.6) will have a nonempty intersection with U_0. Hence we have to use another method of checking if $\varphi(\hat{\mathbf{x}}, (0, t_1]) \subset U_+$. First we compute $\hat{\mathbf{y}} = \hat{\varphi}(\hat{\mathbf{x}}, [0, t_1])$ and then we check if $\hat{\mathbf{y}}$ belongs to the regions where the first state variable x increases. In order to do that, one can compute $\hat{\mathbf{z}} = \hat{\mathbf{A}}_1\hat{\mathbf{y}} + \hat{\mathbf{v}}_1$ and check if points from the set $\hat{\mathbf{z}}$ have the first coordinate positive ($\hat{\mathbf{z}}^T\mathbf{e}_1 > 0$, where $\mathbf{e}_1 = (1, 0, 0)^T$). This can be done by the procedure below.

```
begin
    choose t₁ > 0;
    repeat
```

```
        t₁ = t₁/2;
        ŷ = φ̂(x̂, [0, t₁]);
        ẑ = Â₁ŷ + v̂₁;
    until (inf(ẑᵀe₁) > 0);
end;
```

(2) Find maximum t_2 such that $\varphi(\hat{\mathbf{x}}, (0, t_2])$ is enclosed in U_+. First we choose Δ_t and we set the initial values $t_{\min} = t_1$ and $t_{\max} = t_1 + \Delta_t$. If $\hat{\varphi}(\hat{\mathbf{x}}, [t_{\min}, t_{\max}]) \subset U_+$ then we increase $t_{\min}$ to the value of $t_{\max}$. In the opposite case we decrease Δ_t and repeat checking of the condition. The procedure is continued while Δ_t is greater than some positive number ε_1.

```
begin
    choose Δₜ > 0;
    tₘᵢₙ = t₁;
    while Δₜ > ε₁ do begin
        tₘₐₓ = tₘᵢₙ + Δₜ;
        ŷ = φ̂(x̂, [tₘᵢₙ, tₘₐₓ]);
        if (inf(ŷᵀe₁) > 1) then begin
            Δₜ = 1.5 * Δₜ;
            tₘᵢₙ = tₘₐₓ;
        end
        else Δₜ = Δₜ/1.5;
    end;
    t₂ = tₘᵢₙ;
end;
```

In this procedure it is checked for the subsequent intervals $[t_{\min}, t_{\max}]$, if $\hat{\varphi}(\hat{\mathbf{x}}, [t_{\min}, t_{\max}]) \subset U_+$. $t_{\min}$ is increased only when this condition is fulfilled. As subsequent intervals $[t_{\min}, t_{\max}]$ cover the interval $[t_1, t_2]$ we conclude that $\varphi(\hat{\mathbf{x}}, [t_1, t_2]) \subset U_+$.

(3) Computation of minimum $t_3 > t_2$ such that $\varphi(\hat{\mathbf{x}}, t_3)$ is enclosed in U_0. This procedure is composed of two parts. In the first one we look for any $t_3 > t_2$ fulfilling this condition, while in the second one the value of t_3 is minimized.

```
begin
    choose Δₜ > 0;
    t₃ = t₂;
    repeat
        Δₜ = 1.5 * Δₜ;
        t₃ = t₃ + Δₜ;
        ŷ = φ̂(x̂, t₃);
    until (sup(ŷᵀe₁) < 1);
    {minimization of t₃}
    tₘᵢₙ = t₂;
    tₘₐₓ = t₃;
```

while $(t_{\max} - t_{\min} < \varepsilon_2)$ **do begin**
$\quad t_{\text{med}} = (t_{\min} + t_{\max})/2;$
$\quad \hat{\mathbf{y}} = \hat{\varphi}(\hat{\mathbf{x}}, t_{\text{med}});$
$\quad$ **if** $(\sup(\hat{\mathbf{y}}^T \mathbf{e}_1) < 1)$
$\quad$ **then** $t_{\max} = t_{\text{med}}$
$\quad$ **else** $t_{\min} = t_{\text{med}};$
end;
$\quad t_3 = t_{\max};$
end;

(4) As $\hat{\varphi}(\hat{\mathbf{x}}, (0, t_2])$ is enclosed in U_+ and $\hat{\varphi}(\hat{\mathbf{x}}, t_3)$ is enclosed in U_0 the set $\hat{\varphi}(\hat{\mathbf{x}}, [t_2, t_3])$ contains the image of the set $\hat{\mathbf{x}}$ under the Poincaré map. Hence the return time belongs to the interval $\hat{t} = [t_2, t_3]$.

(5) In order to check the continuity of the Poincaré map one has to check the following condition. If the state variable x decreases on the set $\hat{\varphi}(\hat{\mathbf{x}}, [t_2, t_3])$ (i.e. the vector field has nonzero component in the direction of x axis) then the plane $x = 1$ is transversal to the flow on $\mathbf{P}(\hat{\mathbf{x}})$. In this case the Poincaré map is continuous on $\hat{\mathbf{x}}$.

Computation of an image of the set under Poincaré map

When the procedure for return time is ready, the computation of the Poincaré map is easy. Let us assume that $\hat{\mathbf{x}}$ is a rectangle enclosed in the plane $V_+ = \{(x, y, z)^T : x = 1\}$. Let us also assume that this interval is enclosed in the part of V_+ with negative component of vector field in the direction of the x axis. The full Poincaré map $\mathbf{P}$ can be decomposed into two halfmaps $\mathbf{P}_1$, $\mathbf{P}_2$. The first map corresponds to passing through U_0, while the second one corresponds to passing through U_+. First we find the return time $\hat{t}_0 = [t_{0\,\min}, t_{0\,\max}]$ of trajectories starting from $\hat{\mathbf{x}}$ to the plane $x = 1$. The image of $\hat{\mathbf{x}}$ under the first halfmap can be found using the following formula:

$$\hat{\mathbf{P}}_1(\hat{\mathbf{x}}) := \hat{\varphi}(\hat{\mathbf{x}}, \hat{t}_0) = e^{\hat{\mathbf{A}}_0 \hat{t}_0}(\hat{\mathbf{x}} - \hat{\mathbf{p}}_0) + \hat{\mathbf{p}}_0. \quad \text{(A.7)}$$

$\hat{\mathbf{P}}_1(\hat{\mathbf{x}})$ is a rectangle containing the image of $\hat{\mathbf{x}}$ under $\mathbf{P}_1$. Then we find the return time $t_1 = [t_{1\,\min}, t_{1\,\max}]$ of trajectories starting from $\hat{\mathbf{P}}_1(\hat{\mathbf{x}})$ to the plane V_+ after passing through U_+ and we compute the image of $\mathbf{x}$ under full Poincaré map

$$\hat{\mathbf{P}}(\hat{\mathbf{x}}) = \hat{\mathbf{P}}_2(\hat{\mathbf{P}}_1(\hat{\mathbf{x}})) = \hat{\varphi}(\hat{\mathbf{P}}_1(\hat{\mathbf{x}}), t_1)$$
$$= e^{\hat{\mathbf{A}}_1 \hat{t}_1}(\hat{\mathbf{P}}_1(\hat{\mathbf{x}}) - \hat{\mathbf{p}}_1) + \hat{\mathbf{p}}_1.$$

$$\text{(A.8)}$$